

## Two-Dimensional Electronic Conjugation: Cooperative Folding and Fluorescence Switching

Xuan Jiang, John C. Bollinger, and Dongwhan Lee\*

Department of Chemistry, Indiana University, 800 East Kirkwood Avenue, Bloomington, Indiana 47405

Received May 16, 2006; E-mail: dongwhan@indiana.edu

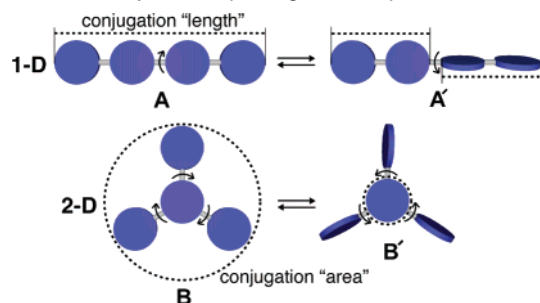
Mechanical control of electronic properties has proven to be an effective signal transduction strategy in molecular-level devices.<sup>1</sup> Linearly  $\pi$ -conjugated “molecular wire” sensors represent one such example, in which binding-induced conformational restriction can significantly modify their emission or conductive properties.<sup>2</sup> Within this context, two-dimensional (2-D)  $\pi$ -conjugations should further benefit from the additional dimensionality of the space sampled by electrons or excited states.<sup>3</sup> The expected decrease in the HOMO–LUMO energy gap would be an additional bonus for their practical applications in sensing and switching with lower energy excitation.

Conceptually intuitive and operationally simple as it might appear, however, the design and implementation of viable switching mechanisms for a planar conjugated system is a formidable synthetic task. As shown in Scheme 1, simple twisting of one bond can effectively change the overall *conjugation length* of a one-dimensional (1-D) system (A), whereas simultaneous rotations of at least three bonds are required to maximize shrinkage and expansion of the *conjugation area* of a 2-D system (B). In this communication, we describe our innovations to meet this challenge by correlating motions occurring at multiple nonproximate locations within dynamic conjugated molecules.

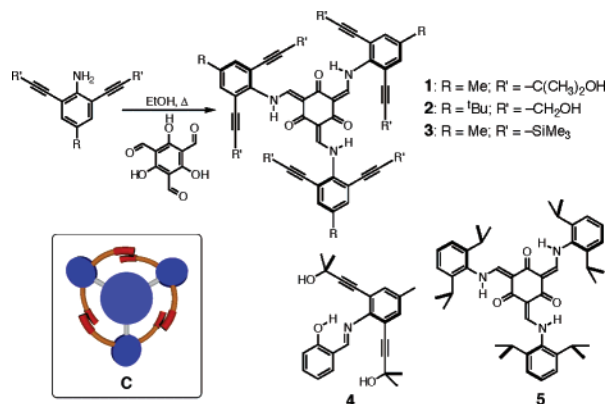
We have recently shown that bulky *m*-terphenyl groups can be placed around a tris(*N*-salicylideneamine) core to furnish shape-adaptive biconcave structures.<sup>4</sup> Within such sterically congested scaffolds, van der Waals contacts facilitate unidirectional tilting of symmetrically disposed aromatic groups. A related structural prototype, represented as C in Scheme 2, was expected to serve as an ideal testbed for the conformational switching depicted in Scheme 1. A convergent synthetic route (Scheme 2) was implemented to furnish compounds 1–5 in efficient two-step sequences from readily available starting materials.<sup>5</sup>

At 25 °C, the <sup>1</sup>H NMR spectrum of 1 in CDCl<sub>3</sub> displayed a sharp O–H resonance at 5.90 ppm, which remained invariant within the concentration range of 2.0–75 mM. The corresponding O–H signal of 4, however, gradually shifted from 2.62 to 3.12 ppm when the concentration was increased from 12 to 210 mM (Figure S1).

**Scheme 1.** Switching in Linear (A and A') and Planar (B and B') Conjugated Systems. Curved Arrows Indicate Rotation about Bonds between Adjacent Repeating Units Represented as Disks



**Scheme 2.** Synthesis of C<sub>3</sub>-Symmetric Switch, Schematically Represented as C, and Its Derivatives



Concentration independence of the significantly downfield-shifted O–H proton resonance of 1 indicated the presence of strong intramolecular hydrogen bonds, which was unambiguously confirmed by X-ray crystallography.

As shown in Figure 1, the planar {C<sub>6</sub>O<sub>3</sub>(CHNH)<sub>3</sub>} core of 1 is surrounded by three aryl groups that are related by crystallographic 3-fold symmetry. The tertiary alcohol groups extending from each of the six ethynyl units engage in O–H···O hydrogen bonding interactions that bring pairs of neighboring “wing tips” to close proximity to define a propeller-like arrangement. These polar interactions extend further to form three O<sub>alcohol</sub>–H···O<sub>alcohol</sub>–H···O<sub>ketone</sub>···H–N<sub>enamine</sub> networks, which converge at the center of the molecule (dotted lines, Figure 1a). Overall, nine X–H···Y (X = O, N; Y = O) bonds effectively flatten and rigidify the entire molecule 1 (Figure 1b).

In CHCl<sub>3</sub> at 25 °C, 1 displays intense ( $\epsilon \sim 7.6 \times 10^4 \text{ M}^{-1} \text{ cm}^{-1}$ ) absorptions at  $\lambda_{\text{max}} = 415$  and 432 nm, which are significantly red-shifted compared with that of its model compound 4 ( $\lambda_{\text{max}} = 350$  nm) or its analogue 5 ( $\lambda_{\text{max}} = 360$  nm) having smaller  $[\pi, \pi]/[n, \pi]$ -

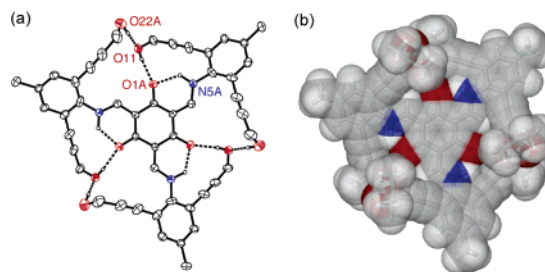


**Figure 1.** X-ray structure of 1: (a) ORTEP diagram with thermal ellipsoids at 50% probability, in which carbon atoms of the *gem*-dimethyl groups and all the hydrogen atoms except O–H and N–H have been omitted for clarity; (b) space-filling model, where N is blue and O is red. Selected interatomic distances (Å): O1A···N5A, 2.634; O1A···O11, 2.765; O11···O22A, 2.809. The {C<sub>6</sub>O<sub>3</sub>(CHNH)<sub>3</sub>} core is disordered over two positions,<sup>5</sup> for which only one model is shown.

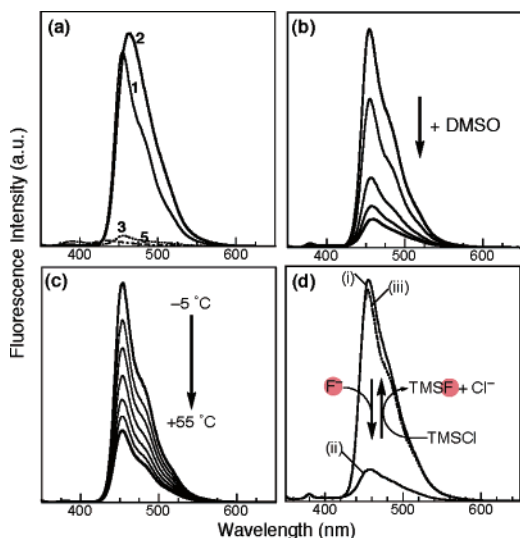


**Figure 2.** Emission spectra of (a) **1**, **2**, **3**, and **5** in  $\text{CHCl}_3$  normalized with absorption at 340 nm; (b) **1** in  $\text{CHCl}_3$ -DMSO with increasing volume fraction of DMSO (0, 20, 40, 60, and 96%, v/v); (c) **1** in  $\text{CHCl}_3$  measured as a function of temperature from  $-5$  to  $+55$  °C with an increment of 10 °C between traces; (d) **2** ( $=1.3$   $\mu\text{M}$ ) in  $\text{CH}_2\text{Cl}_2$  (i) before and (ii) after addition of  ${}^n\text{Bu}_4\text{NF}$  (60 equiv), and (iii) after treatment of (ii) with  $\text{Me}_3\text{SiCl}$  (7.8 mM),  $\lambda_{\text{exc}} = 340$  nm,  $T = 25$  °C.

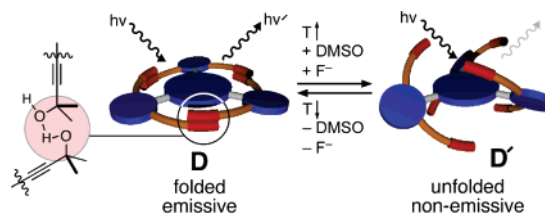
conjugation areas (Figure S2). Upon excitation at 340 nm, **1** displays blue emission at  $\lambda_{\text{max,em}} = 454$  nm with  $\Phi_{\text{F}} = 5.3\%$ . The Stokes shift ( $\Delta\lambda = 22$  nm) of **1** is significantly smaller than that ( $\Delta\lambda = 73$  nm) of **5** with  $\lambda_{\text{max,em}} = 433$  nm, presumably due to the mechanically interlocked hydrogen bonding network which suppresses structural reorganization in the excited states.<sup>6</sup> This structure–property relationship was explored with a set of compounds that share a common tris(*N*-salicylideneaniline) skeleton but differ in the peripheral functionalities.

As shown in Figure 2a, removal of the methyl groups encapsulating the  $\text{O}_{\text{alcohol}}\text{---H}\cdots\text{O}_{\text{alcohol}}\text{---H}\cdots\text{O}_{\text{ketone}}$  linkages (**1**  $\rightarrow$  **2**) has negligible influence on the emission efficiency, whereas complete elimination of this polar network to “loosen” the structure (**1** or **2**  $\rightarrow$  **3** or **5**) quenches the fluorescence. Interaction of **1** with externally added hydrogen bonding solvent, such as DMSO, elicited similar effects (Figure 2b). In contrast, the emission spectrum of **3** lacking this peripheral polar network remained essentially unchanged in response to DMSO. From these observations emerges a simple binary switching model shown in Scheme 3.

Solution dynamics relating **D** and **D'** (Scheme 3) was initially hinted by variable-temperature (VT)  ${}^1\text{H}$  NMR spectroscopy of **1** in  $\text{CDCl}_3$ , in which the O–H proton resonance reversibly shifted as a function of temperature (Figure S3).<sup>7,8</sup> As the temperature was raised from  $-45$  to  $55$  °C, the O–H proton signal of **1** systematically moved upfield from 6.39 to 5.66 ppm in response to the increasing solution population of non-hydrogen-bonded **D'**. This interpretation is corroborated by the VT fluorescence spectra of **1** in  $\text{CHCl}_3$  (Figure 2c), in which loss of hydrogen bonding at higher temperatures facilitates relaxation of the excited states through internal torsional motions within **D'**.<sup>6</sup>

The reversible conformational switching between **D** and **D'** prompted us to drive this process through molecular recognition events. A chemical system was desired that can effectively compete against the intramolecular hydrogen bonding network. The strong hydrogen bonding acceptor ability of the fluoride ion became particularly attractive in this context.<sup>9</sup> At 25 °C, addition of  ${}^n\text{Bu}_4\text{NF}$  (60 equiv) to a  $\text{CH}_2\text{Cl}_2$  solution of **2** immediately quenched the emission (Figure 2d).<sup>10</sup> Subsequent treatment of this mixture

**Scheme 3.** Conformational Switching



with  $\text{Me}_3\text{SiCl}$ , added to scavenge fluoride ion, restored  $>95\%$  of the original fluorescence intensity,<sup>11</sup> thus convincingly demonstrating the reversible nature of this sensing event. Other halide ions, added as  ${}^n\text{Bu}_4\text{NX}$  ( $X = \text{Cl}^-$ ,  $\text{Br}^-$ , or  $\text{I}^-$ ; 60 equiv), had no effects on the emission spectra of **2**. Under similar conditions, **1** did not respond to  $\text{F}^-$  (Figure S4), presumably due to limited access to the sterically more shielded O–H $\cdots$ O units.

In summary, fast and reversible conformational switching of a 2-D conjugated system was achieved by manipulating a mutually reinforcing hydrogen bonding network. Similarly to naturally occurring assemblies that fold cooperatively,<sup>12</sup> individually weak but collectively strong noncovalent interactions could further be reinforced by their symmetric arrangement within a flexible structural scaffold. Folding and unfolding motions of our synthetic constructs are tightly coupled to changes in their emission properties, the technological implications of which are currently being explored.

**Acknowledgment.** This work was supported by Indiana University, the National Science Foundation (CAREER CHE 0547251), and the American Chemical Society Petroleum Research Fund (42791-G3).

**Supporting Information Available:** Experimental details (PDF) and crystallographic data (CIF). This material is available free of charge via the Internet at <http://pubs.acs.org>.

## References

- Balzani, V.; Venturi, M.; Credi, A. *Molecular Devices and Machines: A Journey into the Nanoworld*; Wiley-VCH: Weinheim, Germany, 2003.
- (a) Müllen, K.; Wegner, G. *Electronic Materials: The Oligomer Approach*; Wiley-VCH: New York, 1998. (b) McQuade, D. T.; Pullen, A. E.; Swager, T. M. *Chem. Rev.* **2000**, *100*, 2537–2574. (c) McFarland, S. A.; Finney, N. S. *J. Am. Chem. Soc.* **2001**, *123*, 1260–1261.
- (a) Watson, M. D.; Fechtenkötter, A.; Müllen, K. *Chem. Rev.* **2001**, *101*, 1267–1300. (b) *Chem. Rev.* **2005**, *105*, 3433–3947 (thematic issue on “Delocalization: Pi and Sigma”).
- (a) Riddle, J. A.; Bollinger, J. C.; Lee, D. *Angew. Chem., Int. Ed.* **2005**, *44*, 6689–6693. (b) Riddle, J. A.; Lathrop, S. P.; Bollinger, J. C.; Lee, D. *J. Am. Chem. Soc.* **2006**, ASAP.
- See Supporting Information.
- Valeur, B. *Molecular Fluorescence: Principles and Applications*; Wiley-VCH: Weinheim, Germany, 2002.
- This spectral behavior could best be explained by invoking conformational distribution that is established rapidly on the NMR time scale to provide a single chemical shift reflecting weight-averaged contributions of hydrogen-bonded (**D**) and non-hydrogen-bonded (**D'**) conformers.<sup>8</sup>
- (a) Connors, K. A. *Binding Constants: The Measurement of Molecular Complex Stability*; Wiley: New York, 1987. (b) Gellman, S. H.; Adams, B. R.; Dado, G. P. *J. Am. Chem. Soc.* **1990**, *112*, 460–461. (c) Maslak, V.; Yan, Z.; Xia, S.; Gallucci, J.; Hadad, C. M.; Badjic, J. D. *J. Am. Chem. Soc.* **2006**, *128*, 5887–5894.
- Beer, P. D.; Gale, P. A. *Angew. Chem., Int. Ed.* **2001**, *40*, 486–516.
- This process is accompanied by the disappearance of the O–H resonance (5.03 ppm) as well as the collapse of the methylene doublet ( $J = 5.6$  Hz, coupled to O–H) to a broad singlet at 4.52 ppm, which reflects dynamic exchange process through interaction between O–H and  $\text{F}^-$ .
- The formation of  $\text{Me}_3\text{SiF}$  as the reaction product was confirmed by both  ${}^{19}\text{F}$  NMR ( $\delta = -158.67$  ppm vs  $\text{CF}_3\text{CO}_2\text{H}$ ) and HR-MS ( $m/z = 92.0456$ ).
- For a recent example of peptide complexes that fold cooperatively through a  $\text{C}_3$ -symmetric hydrogen bonding network, see: Tatko, C. D.; Nanda, V.; Lear, J. D.; DeGrado, W. F. *J. Am. Chem. Soc.* **2006**, *128*, 4170–4171.

JA063413U